Computational Modeling:
A PATH TO EXPAND THE KNOWLEDGE BASE IN FUSION WELDING

T. DebRoy

Aditya Birla Chair, Department of Mechanical Engineering Indian Institute of Science, Bangalore, India
Professor of Materials Science and Engineering
The Pennsylvania State University, University Park, PA, USA

Abstract

Welded joints contain spatial variations of composition, structure and properties that are affected by heat transfer, flow of molten metal in the weld pool and solid state transformations during welding. The main challenge in the control of weld properties originates from the complexity of both the fusion welding processes as well as the welded materials. Solutions of complex welding problems based on scientific principles under the framework of computational modeling are already providing solutions for a variety of problems. Computer models of heat transfer, fluid flow and thermal cycles can now be relied upon to provide fusion zone geometry, temperature fields and thermal cycles with a fair degree of confidence. Significant progress has also been made in building a quantitative understanding of various structural features such as phase composition, grain structure and inclusion structure, mostly for several relatively simple alloys. In order to understand and eventually control welding processes and welded materials, significant expansion of our current quantitative understanding of various aspects of welding is necessary. The expanded knowledge base can serve as a basis for the control of welding processes, greatly enhance the quality, reliability and serviceability of welded structures and transform welding to a mainstream engineering branch. Achievement of this challenging but realistic goal, an important milestone in the advancement of welding technology, is well within the reach of the welding community.

Introduction

In the recent decades, new welding processes such as the friction stir welding and advanced technology such as computer aided welding process control have found increased acceptance in the industry. However, our past success cannot be relied upon as insurance for continued good health and prosperity of our field, since we live in an era of unprecedented technological change. So, what can we do now to maintain and enhance the vitality of welding technology? Certainly, innovations cannot be organized or predicted because of their very nature. However, research and development (R&D) can be organized to provide less radical, but more predictable technological solutions. In practice, reliable welds are often fabricated by trial and error without the use of any organized research. So, does it make sense for the industry to invest in organized R&D? In many instances, systematic R&D can be very useful in seeking solutions where traditional empirical methods fail. For example, the trial and error solutions ignore the potential competitive advantage that is attainable through understanding of the underlying science. Furthermore, multiple work-pieces are not always available. Finally, sometimes the value of the work piece is considerably enhanced prior to welding, making trial and error paradigm expensive.

The main challenge in the control of joint properties originates from the complexity of both the fusion welding processes as well as the welded materials. Welded joints typically contain spatial gradients of composition, structure and properties that are affected by

processes such as the heat transfer, flow of molten metal in the weld pool and solid state transformations during welding. Organized R&D seeks to better understand these complexities and control characteristics of welded materials and processes.

As a result of organized R&D, there is now a growing quantitative knowledge base in welding. Can this knowledge base provide solutions of today's welding problems? The answer depends on the specific solution desired. It is fair to say that it is already providing solutions for a variety of problems[1]. Computer models of heat transfer, fluid flow and thermal cycles can now be relied upon to provide fusion zone geometry, temperature fields and thermal cycles with a fair degree of confidence. Progress has also been made in quantitative understanding of various structural features such as phase composition, grain structure and inclusion structure, mostly for several relatively simple alloys. The goal of this paper is to review a selection of examples where computational modeling has made a significant difference. These examples show that phenomenological modeling can provide insight that cannot be achieved otherwise and the modeling effort can be used to improve weld quality.

1. Weld Metal Geometry

1(a) Role of Surface Active Elements

Beneficial effects of surface active elements, such as sulfur and oxygen, in improving weld

penetration have been known for well over a decade.[2] In many cases, though, the presence of sulfur has not actually resulted in the expected high depth of penetration. For example, cross sections of steel welds containing 20 and 150 ppm of sulfur and laser welded under different powers[3] are shown in Fig. 1(a-d). The pool geometry in each steel is similar in appearance with a laser power of 1900 W. However, when the samples are welded at a laser power of 5200 W, the weld containing 150 ppm sulfur has a much greater depth of penetration than that containing 20 ppm sulfur. Thus, the concentration of sulfur may or may not have a significant effect on the weld geometry under the given range of welding variables.

Why didn't the higher sulfur concentration improve penetration at 1900 W? In general, for counterintuitive results, possible lack of reproducibility of the data cannot be ruled out. However, in this investigation, over eighty experiments were carefully conducted and the results were reproducible. These results lead to an important question: how can we predict and control weld penetration?

The answer to this question requires discussion of numerically computed results and is deferred until the end of this section. We start by examining the relative magnitudes of heat transfer by convection and conduction within the weld pool, which is expressed by the Peclet number for heat transfer, Pe:

$$Pe = \frac{uL}{\alpha} \qquad (1)$$

where u is the velocity, α is the thermal diffusivity of the liquid metal, and L is the characteristic length that can be taken as the depth of the weld pool. In the calculation of Pe, the value of the velocity is required. Fig. 1 shows the computed velocity and temperature fields and the weld geometries.[3] These calculations are based on the solution of the equations of conservation of mass, momentum, and energy in a transient, two-dimensional axi-symmetric form. As shown in each case in Fig. 1, the computed weld geometry agrees well with the corresponding experimental geometry.

At a laser power of 1900 W, the peak temperatures reached on the weld pool surface are both about 1720 K. The relatively low temperature gradients on the weld pool surface lead to low surface velocities. The maximum values of the Peclet number for the steels with 20 and 150 ppm sulfur are 0.18 and 0.91, respectively. These low values of Pe (<1) indicate that heat transfer by conduction is more important than that by convection. As a result, the direction of fluid flow is not important in determining the melting of the base metal and the weld pool shape at this laser power. Consequently, there is no significant difference between the weld pool geometries for steels containing 20 and 150 ppm sulfur. In contrast, at a laser power of 5200 W, the calculated peak temperatures are higher than 2100

K, which produce much more significant temperature gradients and higher surface velocities. The computed Peclet numbers are large (>200), making convective heat transport the primary mechanism for heat transfer.[3] Thus, the fluid flow field and the direction of convective heat transport have a pronounced effect on the weld pool geometry.[3]

The direction of the fluid flow within the weld pool depends on the spatial gradient of interfacial tension, which is the product of the spatial gradient of temperature and the temperature gradient of surface tension, dg/dT. For a sulfur content of 20 ppm, the temperature gradient of surface tension[4,5] is negative at all temperatures. The negative values of dg/dT over the weld pool surface result in radially outward flow over the entire weld pool surface and a shallow weld pool, as shown in Figs. 1(a) and 1(b). When the sulfur content is 150 ppm, dg/dT is positive, which results in a radially inward flow and the convective heat transport in the downward direction near the heat source results in deep pools, as observed in Fig. 1(d). Since dg/dT is negative at temperatures higher than 1980 K for the steel containing 150 ppm sulfur, it generates a radially outward secondary flow in a small region near the middle of the pool. However, this secondary flow is mild and a deep weld pool is obtained at 150 ppm sulfur because of the dominant radially inward flow and high Peclet number.

Only when convection is the dominant mechanism of heat transfer can surface active elements play an important role in enhancing weld penetration. This example shows that numerical calculations of heat transfer and fluid flow can provide detailed insight into welding processes that cannot be achieved otherwise. A well-tested mathematical model, that considers the role of surface active elements such as oxygen and sulfur, can accurately predict weld pool geometry.

1(b) Modeling of "Finger" Penetration in GMA Welding

Weld pools formed during gas metal arc (GMA) welding display a unique shape not commonly observed in other welding processes. These weld pools are characterized by a much deeper penetration,[6] resembling a finger, and is shown in Fig. 2 for several sets of welding parameters. This feature is the result of droplets detaching from the consumable electrode and impinging on the weld metal surface. These droplets aid in the transport of heat, supplementing the energy transfer from the arc. Knowledge of the weld penetration is useful in developing welding procedures to achieve reliable welds without excessive trial and error.

As an example, the evolution of the weld pool geometry during the GMA welding of HSLA-100 steel is examined using the fundamentals of transport phenomena. A three-dimensional turbulent heat transfer model is used here to solve for the equations of conservation of mass, momentum, and energy. In GMA welding, a high level of agitation in the weld pool is aided by both the large mean velocities present in the relatively small weld pool and the impact of the metal droplets from the consumable electrode. Experimental observations[7] and theoretical calculations[8,9] in gas tungsten arc (GTA) welding have indicated that the fluid flow is turbulent in nature. The widely used K-e model[10] has been adopted here to simulate turbulent heat transfer and fluid flow in the weld pool.

The difficulty encountered in the simulation of the GMA welding process involves the transfer of metal drops from the consumable electrode to the weld pool and the resulting heat and momentum transfer. These droplets deliver their excess heat to the molten weld pool and are responsible for the finger penetration observed during the GMA welding process. The heat transfer from the metal droplets has been simulated by considering the existence of a cylindrical volumetric heat source in the weld pool,[6] whose dimensions are determined by the drop size, shape, velocity, and frequency. The procedure for the calculation of the volumetric heat source is available in the literature.[11]

An example of the computed temperature and velocity fields in three dimensions considering turbulent transfer of heat and momentum[6] is shown in Fig. 3. The general features of the calculated temperature fields are consistent with the expected results. For example, temperature gradients

are greater in front of the heat source than behind it. These temperature gradients in front of the heat source result in slightly greater liquid metal velocities here than behind the heat source. The computed weldment geometry[6] is compared with the experimental weld pool shape and size in Fig. 2(a-c) for several welding conditions. It is observed that the width of the fusion zone, the depth of the finger penetration, and the shapes of both the fusion zone and HAZ predicted by the model agree with the corresponding experimental results. Furthermore, "finger" penetration can be satisfactorily predicted using this model. The modeling effort, apart from providing a detailed insight about the physical processes in GMA welding, can reduce the volume of experiments needed to develop welding protocol for a given application.

The modeling efforts can provide geometric information in both linear[12-14] as well as spot welding, [15,16] in complex geometries such as fillet welding[17] and in systems with considerable surface deformation.

2. Quantitative Understanding of Weldment Structure

Quantitative prediction of the role of welding variables on the weld metal structure is now possible for many important metals and alloys. A few case studies, which use mathematical modeling to calculate structural characteristics of the weldment are described here. For example, modeling can be useful in revealing the phase transformation mechanisms in commercially pure titanium. Modeling is also applied to understand the evolution of grain structure under steep temperature gradients during welding of titanium. Computer modeling has also been used to simulate the inclusion composition and size distribution in the weld metal considering the nucleation, growth, and dissolution rates of inclusions.

2(a) Understanding Mechanism of Phase Transformations

Phase transformation rates can be expressed by the Johnson-Mehl-Avrami (JMA) equation when the transformations are controlled by the classical nucleation and growth mechanism. The JMA equation can be modified for non-isothermal kinetics, and the detailed procedure to derive the modified JMA equation is available in the literature.[18] This method uses a discretization of the time dependence of temperature by approximating the continuous temperature-time curves by many isothermal steps. The final expression for the transformed fraction obtained from m subsequent isothermal steps is expressed in the following relationship:

$$f(t(T)) = 1 - \exp\left\{-\left[\sum_{l=0}^{m-1} k(T_0 + l\Delta T)\Delta t\right]^n\right\} \quad (2)$$

were f(t(T)) is the transformed phase fraction under non-isothermal conditions, Dt is the time step, DT is the temperature change corresponding to each Dt, T_0 is the initial temperature, k is a time dependent constant, and m is the total number of the isothermal steps. The parameters, k and n, depend on the mechanism of the phase transformation.

During welding of commercially pure titanium,[19] the fusion zone undergoes a transformation from the a to the b to the liquid and back through the b to the a phase. The heat affected zone (HAZ) goes from the a to the b and back to the a phase. The extent of the phase transformation in the HAZ and the times for the completion of the a®b transition for each assumed transition mechanism can be calculated from the knowledge of the thermal cycles. These calculated times for each mechanism are then compared with the times determined from the experimental phase distribution map in Fig. 4. There is good agreement between the times taken from the phase distribution map and those calculated assuming that the a®b transition is controlled by the transport of Ti atoms across the interface and it may be assumed here that the a®b transition is primarily controlled by the transport of Ti atoms across the interface (mechanism I).[19] The use of mathematical modeling here produces knowledge of phase transformation mechanism, which can not be achieved with experiments alone.

2(b) Modeling of Grain Growth in the HAZ

In recent years, modeling of grain growth has greatly aided our understanding of grain structure evolution during welding. In the past, Monte Carlo (MC) techniques

have been used to simulate the evolution of grain structure under isothermal conditions[20-23] and recently the technique has been applied to the HAZ of welds[19,23-25] where the steep temperature gradients near the fusion zone have been taken into account.

The evolution of grain structure within the HAZ has been recently modeled in three dimensions using a Monte Carlo technique.[19] By incorporating the calculated thermal history data obtained from a well-tested heat transfer and fluid flow model, the simulated grain growth kinetics at each site can be calculated. The simulated final grain structure in the HAZ[19] is shown in Fig. 5. Significant spatial grain size gradients are observed in the simulated HAZ structure. At sites closer to the fusion line, the grains are coarser, since the grain size change depends on both the temperature and time period for grain growth. It is also observed that grain growth on the top surface of the HAZ (line ab) is less than that observed in the vertical direction (line cd). The calculated and experimental grain sizes were found to be comparable.[19] In recent years, advancements in computational modeling have provided significant insight into the evolution of structure in welded materials. The feasibility of calculating the evolution of grain growth in three dimensions, demonstrated by the example presented here, represents a new tool for quantitative understanding of the structure of welded materials.

2(c) Modeling of Inclusion Characteristics

The rate of precipitation of inclusions from a supersaturated solution can be determined from the rate of diffusion of their constituent elements to the inclusion surface where the growth takes place.[26,27] In the weld pool, the inclusions experience considerable recirculatory motion[28,29] and strong temperature gyrations along their path. It has been recently shown that[28,29] our current knowledge of heat transfer and fluid flow in the weld pool can be utilized to understand the growth and dissolution of solid inclusions in the weld pool. The loci and the temperature gyrations experienced by a large number of inclusions have been calculated numerically to seek a statistically meaningful residence time distribution for the inclusions and the number and the intensities of the temperature cycles experienced by these particles.

A typical computed temperature versus time plot and the corresponding Al_2O_3 inclusion radius versus time plot are shown in Fig. 6 for the SMA welding of a low alloy steel.[29] It can be seen that these inclusions begin to dissolve above about 2210 K and grow again when the temperature falls below this level. Its radius reaches about 1 mm before it is lodged in the solidified weld metal. Calculations show that the majority of the inclusions undergo some dissolution within the weld pool during their life cycle. The coarsening of the inclusions is facilitated by the longer times available at low welding speeds. Furthermore, the size distribution

curves become flatter when the welding velocity decreases. The computed and measured size distributions are presented in Fig. 7 as a plot of radius versus percentage of particles. Good agreement[29] between the computed and the measured values indicates that important aspects of weld metal structure can be understood from the fundamentals of transport phenomena and kinetics.

Concluding Remarks

In recent years, phenomenological modeling has provided significant insight into fusion welding processes and weldment characteristics which could not have been obtained solely through experiments. The examples presented in this paper demonstrate how significant insight can be achieved by using large phenomenological models that contain detailed description of important physical processes.

Comprehensive phenomenological models are not widely used by practicing welding engineers today since they are complex and computationally intensive. A practical solution for facilitating the use of numerical models is to develop relatively simple process control models, such as neural networks. These models do not consider any of the physical processes in welding, and as a consequence, are computationally simple and can be used in real time. However, development of these simple models requires an extensive data base. In addition to experimental results, some of the

necessary data can be generated by the comprehensive phenomenological models. The large models can be used to calibrate, train, and verify, the simple, real-time, process control models. Thus, apart from providing insight into welding processes, phenomenological models are also potentially useful for the development of process control models. Improved user access to the large models at low cost would also be helpful in gaining wider acceptability of the models.

In addition to being potentially more useful to practicing engineers, phenomenological models are a powerful tool for research today. Modeling of weldment geometry and structure, presented here, represents a small contribution to an expanding quantitative knowledge base in welding. Significant expansion of this knowledge base is necessary, if not essential, for transforming welding from almost an empirical art to an engineering science.

References

1. T. DebRoy and S.A. David, Reviews of Modern Physics, 1995, 67(1), 85.

2. C. R. Heiple and J. R. Roper, Weld. J., 1982, 61, 92s-101s.

3. W. Pitscheneder, T. DebRoy, K. Mundra, and R. Ebner, Weld. J., 1996, 75(3), 71s -80s.

4. P. Sahoo, T. DebRoy and M.J. McNallan, Metall. Trans. B, 1988, 19B, 483-491.

5. M. J. McNallan and T. DebRoy, Metall. Trans. B, 1991, 22B, 557-560.

6. Z. Yang and T. DebRoy, Metall. Mater. Trans. B, 1999, 30, 483-493.

7. M. Malinowski-Bodnicka, G. den Ouden and W.J.P. Vink, Weld. J., 1990, 69, 52s-59s.

8. R.T.C. Choo and J. Szekely, Weld. J., 1994, 73(2), 25s-31s.

9. K. Hong, D.C. Weckman and A.B. Strong in Trends in Welding Research, H.B. Smartt, J.A. Johnson, and S.A. David, eds., ASM

International, Materials Park, OH, 1996, 399-404.

10. B.E. Launder and B.D. Spalding, Mathematical Models of Turbulence, Academic Press, New York, NY, 1972.

11. S. Kumar and S.C. Bhaduri, Metall. Mater. Trans. B, 1994, 25B, 435-41.

12. H. Zhao and T. DebRoy, Journal of Applied Physics, 2003, 93(12), 10089-10096.

13. J. W. Elmer, T. A. Palmer, W. Zhang, B. Wood, and T. DebRoy, Acta Materialia, 2003, 51(12), 3333-3349.

14. S. A. David, R. Trivedi, M. E. Eshelman, J. M. Vitek, S. S. Babu, T. Hong and T. DebRoy, Journal of Applied Physics, 2003, 93(8), 4885-4895.

15. X. He, P. W. Fuerschbach and T. DebRoy, Journal of Physics, D: Applied Physics, 2003, 36, 1388-1398.

16. W. Zhang, G. Roy, J. Elmer and T. DebRoy, Journal of Applied Physics, 2003, 93(5), 3022-3033.

17. C.-H. Kim, W. Zhang and T. DebRoy, accepted for publication in Journal of Applied Physics.

18. P. Kruger, J. Phys. Chem. Solids, 1993, 54(11), 1549.

19. Z. Yang, J.W. Elmer, J. Wong, and T. DebRoy, Weld. J. 2000, 79(4), 97s-112s.

20. M.P. Anderson, D.J. Srolovitz, G.S. Grest, and P.S. Sahni, Acta Metall., 1984, 32, 783-791.

21. D.J. Srolovitz, M.P. Anderson, P.S. Sahni, and G.S. Grest, Acta Metall., 1984, 32, 793-802.

22. Y. Saito and M. Enomoto, ISIJ International, 1992, 32, 267-274.

23. J. Gao and R.G. Thompson, Acta Metall., 1996, 44, 4565-4570.

24. Z. Yang, S. Sista, J. W. Elmer, and T. DebRoy, Acta Materialea, 2000, 48(20), 4813-4825.

25. S. Sista, Z. Yang and T. DebRoy, Metallurgical and Materials Transactions B, 2000, 31B, 529-536.

26. T. Hong and T. DebRoy, Ironmaking and Steelmaking, 2001, 28(6), 450-454.

27. T. Hong and T. DebRoy, Metallurgical and Materials Transactions B, 2003, 34B, 267-269.

28. T. Hong, W. Pitscheneder and T. DebRoy, Science and Technology of Welding and Joining, 1996, 3(1), 33-41.

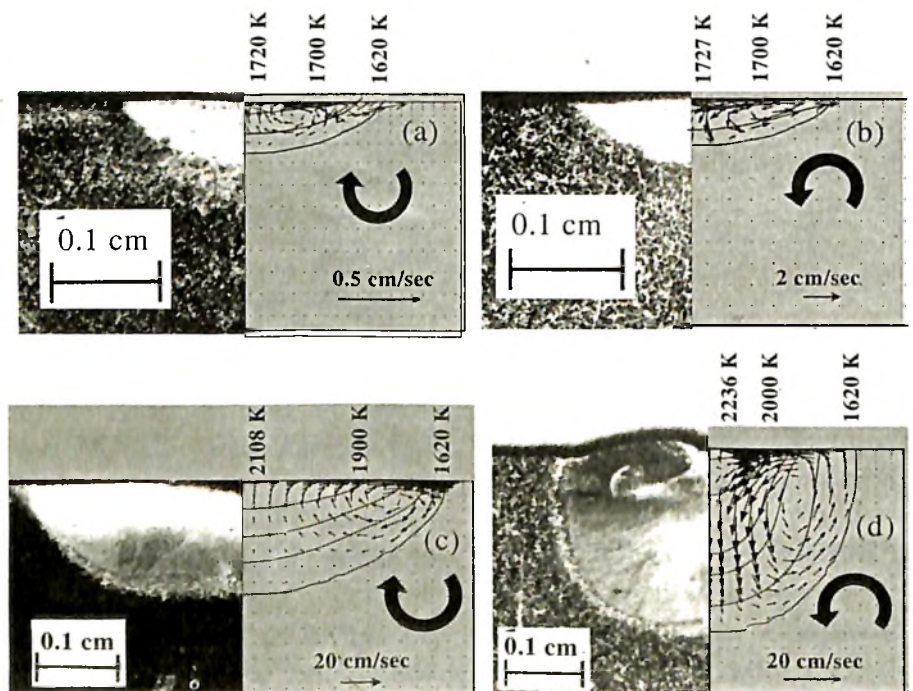T. Hong, T. DebRoy, S. Babu and S. A. David, Metall. and Mat. Trans. B, 2000, 31B, 161-169.

Figure 1(a-d). Comparison between the computed and experimental weld pool geometry[3] at a laser power of 1900 W for steels containing (a) 50 ppm and (b) 150 ppm sulfur and at a laser power of 5200 W for steels containing (c) 50 ppm and (d) 150 ppm sulfur.
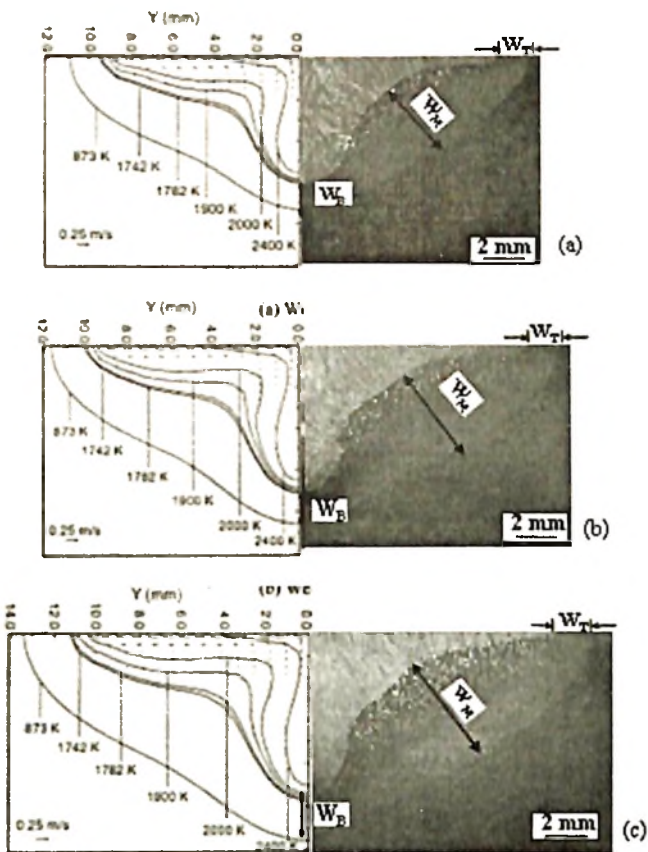
Figure 2(a-c). Comparison of the calculated and experimental geometry of the fusion zone and the HAZ. The conditions for the three welds shown are defined elsewhere.[6] The heat input per unit length for the three welds is: (a) weld 3: 2.4 kJ/mm, (b) weld 2: 3.15 kJ/mm, and (c) weld1: 3.94 kJ/mm. The symbols W_T, W_M, and W_B are the widths at the top, middle, and bottom of the HAZ.[6]
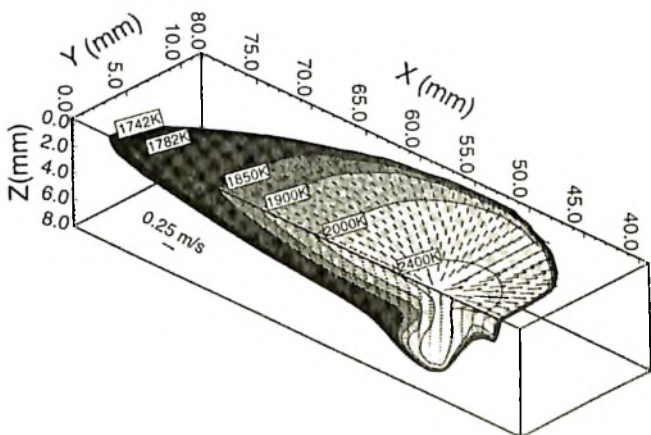

Figure 3. Calculated temperature and velocity fields in GMA welded HSLA-100 steel with a welding current of 405 A, a welding voltage of 31.3 V, a travel speed of 5.29 mm/sec, and no preheat.[6]
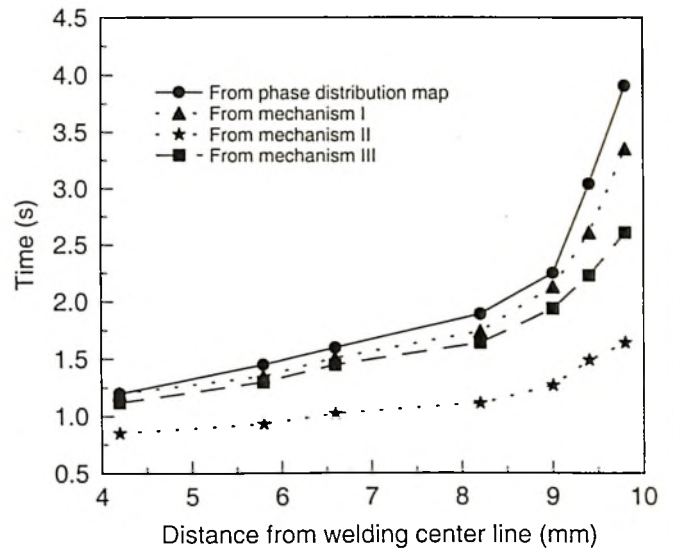
Figure 4. Comparisons of times need for the a®b transformation from the JMA equation and from the phase distribution map. Different mechanisms are assumed for the application of the JMA equations are discussed elsewhere.[19] Mechanism I: Ti short range diffusion, II: oxygen long range diffusion and III: oxygen short range diffusion.
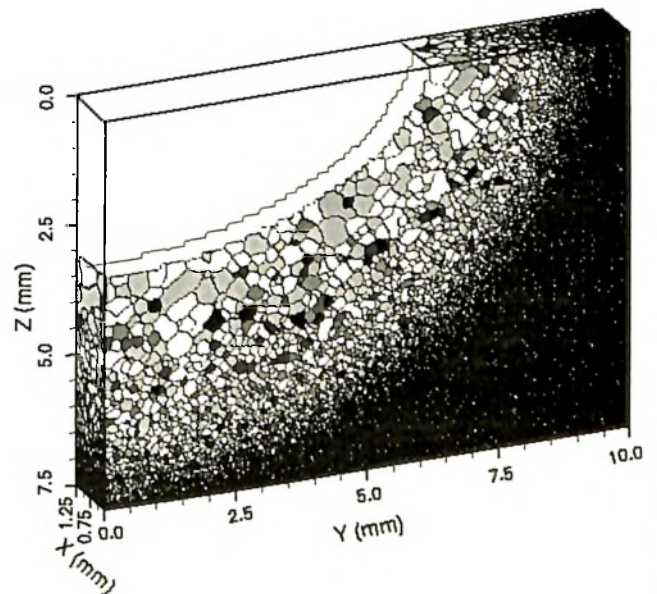

Figure. 5: Three dimensional grain structure of the HAZ of a GTA welded titanium weldment computed using 3D temperature field from the heat transfer and fluid flow model.[19]
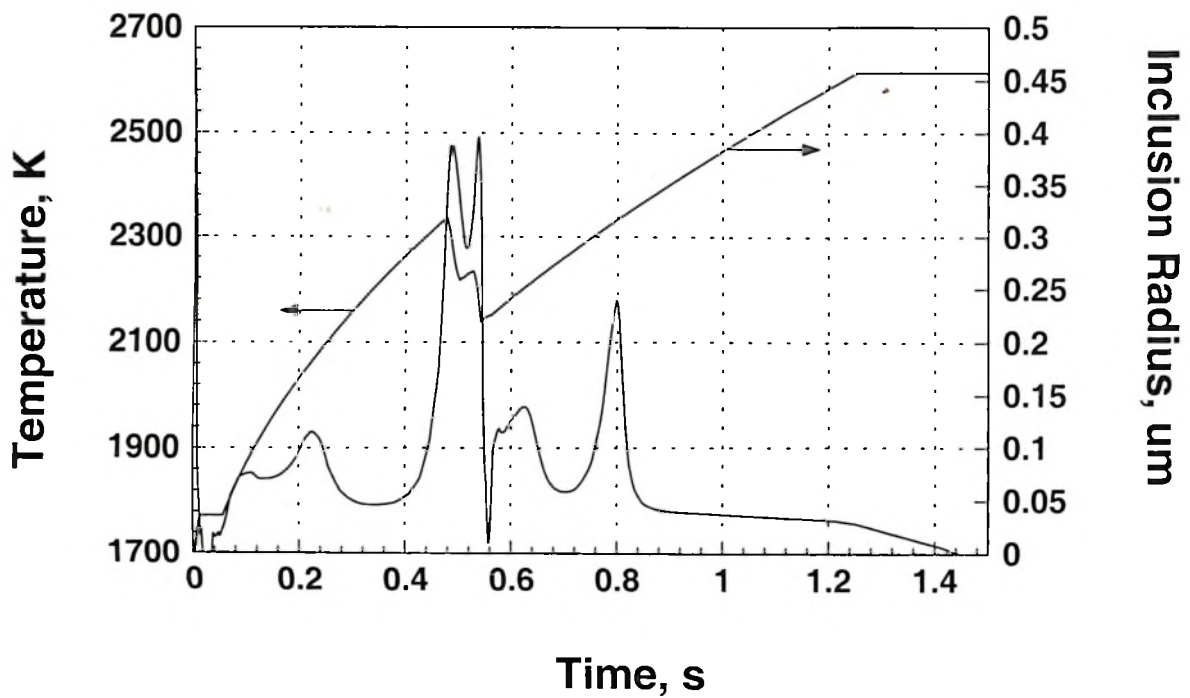
Figure 6. A typical temperature gyration experienced by an inclusion and the corresponding size change in the weld pool.[29]
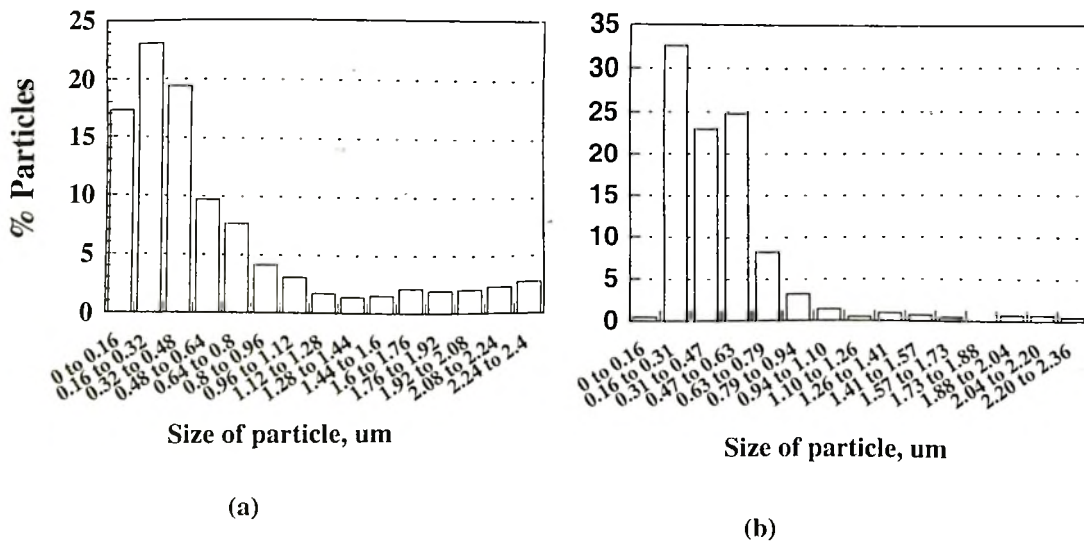

(a)

(b)

Figure 7. (a) Computed inclusion size distribution.[29]
(b) Experimental inclusion size distribution in a controlled experiment.[29]